The Resolution Function of the Chopper Spectrometer HET at ISIS

T.G. Perring

ISIS Facility, Rutherford Appleton Laboratory,
Chilton, nr. Didcot, Oxon OX11 OQX, U.K.

0. ABSTRACT

The calculation of the resolution function of the chopper spectrometer HET at high incident neutron energies is described. The method is to calculate the *inverse* of the Cooper-Nathans resolution matrix, which can be achieved with much less algebra than a conventional calculation of the resolution function. A simplified version of the calculation is used to predict monitor widths, from which the moderator pulse width is parameterised and found to be much broader than expected. The data is used with the full calculation to predict linewidths of scattered neutron peaks from vanadium which are compared with experimental data. Comparison between inelastic data from single crystal MnCu and the 4-D convolution of the resolution function with a model dispersion relation is presented, which show good agreement.

1. INTRODUCTION

When any inelastic spectrometer is set up to observe a point $(\underline{Q}_0,\omega_0)$ in reciprocal space the spectrometer in fact accesses a region of $(\underline{Q},\omega)$-space due to the spread of incident and final wavevectors about their nominal values. On a triple-axis spectrometer the spread arises from the range of angles that the collimators pass and the mosaic spreads of the monochromating and analysing crystals. In the case of a time-of-flight chopper spectrometer (TOFCS) the spread arises not only from the geometric collimation from the sizes of the moderator, sample and detector, but also from the distribution of flight-paths and the time-widths of the pulses from the moderator and chopper.

The resolution function for a triple-axis spectrometer is known to be a highly correlated function in $(\underline{Q},\omega)$-space, broad in some directions but close to singular in others. This is also the case for a TOFCS. A knowledge of the form of the resolution function is important in scattering experiments from single crystals to match the resolution widths

with the problem being investigated, to focus peaks (minimise the width and maximise the height), and to determine if observed peaks widths are intrinsic to the scattering function. In section 2 the formalism of the resolution function calculation for HET is outlined and general features of the function discussed. In section 3 comparison is made between calculation and observed widths in direct-beam monitors and vanadium scattering to the detectors, and in section 4 an example of the simulation of HET data from a single crystal is presented.

2. FORMALISM

In figure 1 a schematic picture of the HET spectrometer [1] is shown. In the equations below, the arguments of the functions are deviations in time or distance from the values for the 'nominal' neutron. This neutron leaves the moderator face with wavevector $\underline{k}_I$, as determined from the first moments in two monitors placed in the beam behind the Fermi chopper, passes throught the chopper when the slits are parallel with the spectrometer axis, are scattered with final wavevector $\underline{k}_F$ and absorbed at the centre of the detector. The infinitesimal intensity can be written as

$$dI = [\phi(k_i)M(t_m)dy_m dz_m d^3\underline{k}_i dt_m][A(y_a)A_z(z_a)P(t_{ch}+\frac{u}{\omega})]$$
$$\times[\frac{\hbar}{mk_i}S(\underline{Q},\omega)s(x,y,z)dxd^3\underline{k}_f][D(x_d,y_d)D_z(z_d)dx_d.T(t_d)dt_d] \qquad [1]$$

Here $\phi(k_i)$ is the flux distribution on the moderator, $M(t_m)$ the pulse shape and $dy_m dz_m$ an element of area on the moderator face. $A(y_a)A_z(z_a)$ is the product of two hat functions that give the transmission through a beam defining aperature about 3m after the moderator, and $P(t'_{ch})$ the pulse shape through the chopper, u the angle of the neutron to the spectrometer axis and ω the angular velocity of the chopper. The third pair of brackets gives the fraction of neutrons scattered by the sample into the phase space element $d^3\underline{k}_f$ by a thickness dx of the sample. The function $s(x,y,z)$ is zero outside the sample volume and which gives the attenuation of the neutron beam when scattered at the point (x,y,z) within the sample. The final term in brackets is the fraction of neutrons absorbed in thickness dx_d in the detector and in time dt_d. $T(t_d)$ is a hat function with width equal to the time channel width. The variables can be changed to those that appear as function arguments to give

$$dI = \left[\frac{\hbar^2}{m^3}\frac{k_f^4 k_i \phi(k_i)}{l_0(l_a+l_1)l_2^3}\right]MAA_z sDD_z T_d dy_a dz_a dt_m dt'_{ch} dt_d\, d^3\underline{r}\, d^3\underline{r}_d.S(\underline{Q},\omega) \qquad [2]$$

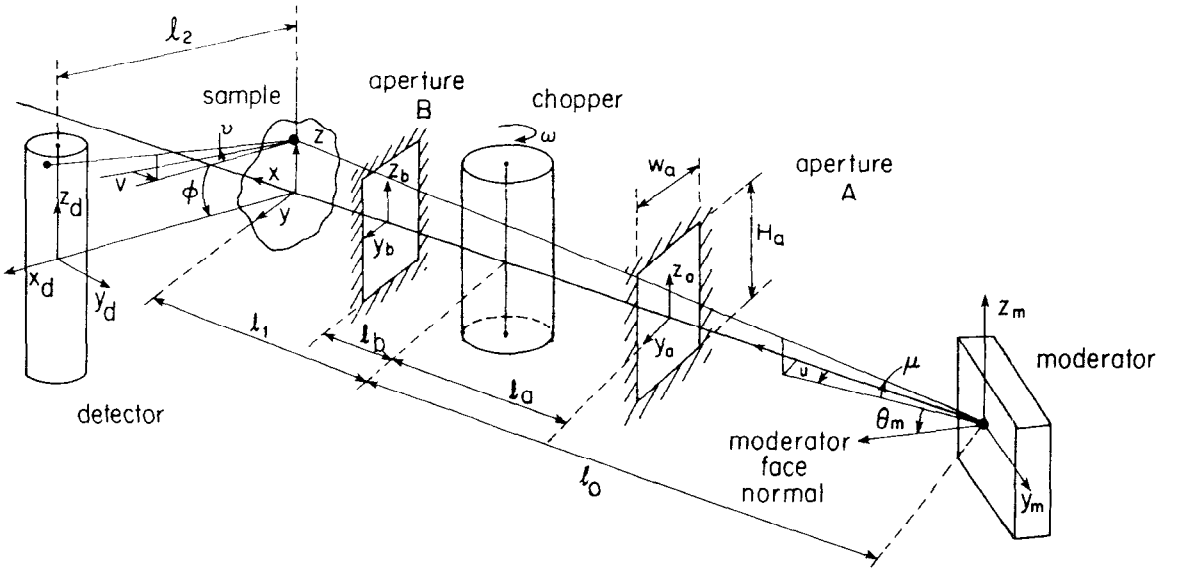

Figure 1: A schematic diagram of the HET spectrometer

where l_0 is the distance between the moderator and the chopper, l_a the distance from the beam defining aperture to the chopper, l_1 the distance from the chopper to the sample and l_2 the sample -detector distance. The integral can be written in the conventional form

$$I(\underline{Q}_0,\omega_0) = \int R\left(\underline{Q}-\underline{Q}_0,\omega-\omega_0\right) S\left(\underline{Q},\omega\right) d\underline{Q}d\omega \qquad [3]$$

where

$$R(\underline{Q}-\underline{Q}_0,\omega-\omega_o) = [\ldots]\int MAA_z sDD_z T_d\, \delta(\underline{Q}-\underline{Q}_0)\delta(\omega-\omega_0)dy_a dz_a \ldots d^3\underline{r}_{\text{det}} \quad [4]$$

In the corresponding treatment of a triple-axis spectrometer the resolution function is approximated by a Gaussian form. This simplification is not generally appropriate for a TOFCS at a pulsed source because of the asymmetry of the moderator pulse. However, at high incident neutron energies the asymmetry in the resolution is small and the approximation is valid. The conventional treatment would be to write each function as a Gaussian, change variables to $\delta\underline{Q} \equiv \underline{Q}-\underline{Q}_0$ and $\delta\omega \equiv \omega-\omega_0$ plus seven others, completing the square and integrating for each of the seven remaining variables in turn. A far simpler and more elegant method is to calculate directly from the integrand the covariance matrix $C_{\alpha\beta} = \left\langle \delta Q_\alpha \delta Q_\beta \right\rangle$, where $\alpha,\beta = 1 \rightarrow 4$ and $\delta Q_4 \equiv \delta\omega$. This is achieved by approximating the deviations δQ_α as a linear combination of the integration variables $\{X_i\} \equiv (y_a, z_a \ldots d^3\underline{r}_d)$ so that $\delta Q_\alpha = T_{\alpha j} X_j$, when

$$C_{\alpha\beta} = \left\langle \delta Q_\alpha \delta Q_\beta \right\rangle = T_{\alpha j} T_{\beta k} \left\langle X_j X_k \right\rangle \qquad [5]$$

As the integrand is largely the product of functions of one variable, most of the $\langle X_j X_k \rangle$ with $j \neq k$ are zero. The only non-zero off-diagonal elements arise potentially from the sample function $s(x,y,z)$. The diagonal terms are mostly easy to calculate apart from the variance of the depth of absorption in the gas tube detectors, which must be performed numerically. For instance, the pulse from the moderator as high energies can be approximated as [2]

$$M(t_m) = \frac{1}{2\tau^3}(t_m + 3\tau)^2 \exp\left(-\frac{t_m + 3\tau}{\tau}\right) \quad ; \quad \tau = \frac{1}{\Sigma v} \qquad [6]$$

where Σ is the macroscopic cross-section for the moderator material and v is the speed of the neutron. For this expression, $\langle t_m \rangle = 0$ and $\langle t_m^2 \rangle = 3\tau^2$. The variance of the pulse in a Fermi chopper is given in [3]. The resolution function in the Gaussian approximation is then

$$R(\delta\underline{Q}) = \frac{V_{res}}{4\pi^2 |\underline{\underline{C}}|^{\frac{1}{2}}} \exp\left(-\frac{1}{2}(\delta\underline{Q}, \delta\omega) \cdot \underline{\underline{C}}^{-1} \cdot (\delta\underline{Q}, \delta\omega)^T\right) \qquad [7]$$

where V_{res} is the resolution volume, given by the integral of equation 2 with unit $S(\underline{Q},\omega)$. The method is entirely equivalent to that of [4] with $C^{-1}_{\alpha\beta}$ corresponding to the matrix elements $m_{\alpha\beta}$. It should be emphasised that the formalism takes account of all correlations introduced into the resolution function, for instance the sweep of the chopper across the moderator face and the sample, and the energy spread as well as the time spread of neutrons from the moderator that pass through the chopper. The only approximations are the ones usually made in resolution function calculations i.e. the spreads $\delta\underline{Q}$ and $\delta\omega$ are small in comparison to $\underline{k}_i, \underline{k}_f$ and E_i, E_f, and that Gaussian approximations are valid. It is possible to retain asymmetric functions in the formalism at the penalty of considerably more algebra, but this is not required for the high energy case being considered here.

An algorithm to calculate the resolution function according to the above formalism has been incorporated into two computer programs. RESCHOP calculates the resolution function and the peak width from a planar dispersion relation, and is similar in operation to the triple-axis spectrometer program RESCAL available at the ILL and elsewhere; and HETSIM which performs the 4D convolution of the resolution function with a model dispersion relation to simulate the results of a scattering experiment from a single crystal.

For any neutron spectrometer in the small scattering angle limit with small fractional energy transfer (the conditions in high energy magnetic scattering experiments), the resolution function can be shown to be close to singular, with [5]

$$\delta\omega \approx \frac{\hbar}{2m}\left(\underline{k}_i + \underline{k}_f\right)\cdot\delta\underline{Q} \qquad [8]$$

This result is found to be the case for HET, as shown in figure 2. Generally for HET, the fractional energy resolution $\delta\hbar\omega/E_I$ is ≈2.2% FWHH at the elastic line, reducing to 1.5% for full energy transfer. The fractional momentum resolution $\delta Q/k_I$ is about 1% both transverse and longditudinal. The vertical resolution is dominated by the height of the ^{3}He gas detectors, which are mostly 30cm tall and at 4m or 2.5m from the sample.

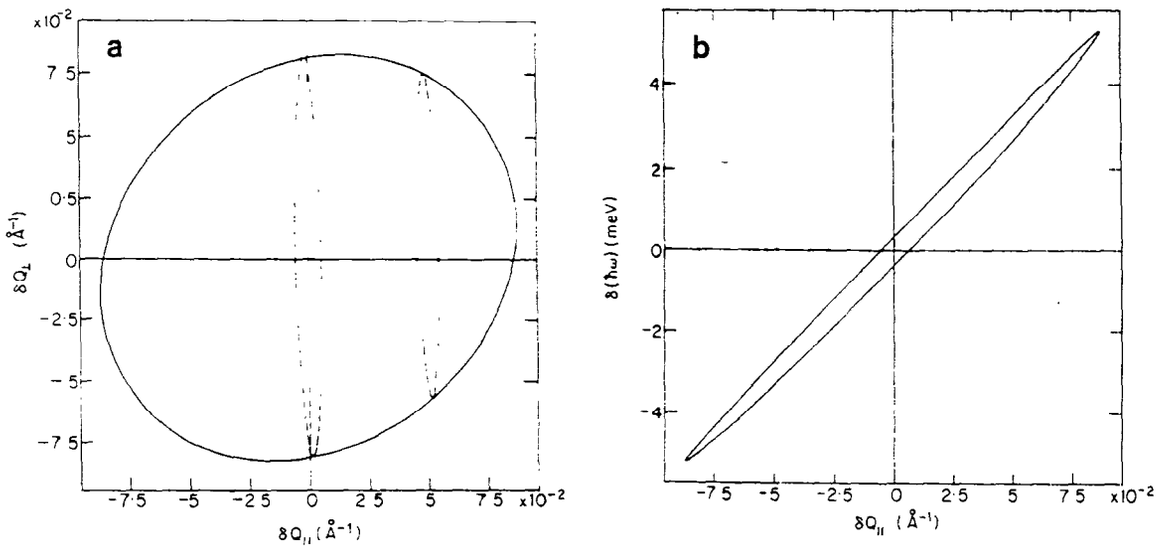

Figure 2: Typical resolution function for HET (E_I =500meV, $\hbar\omega$ = 150meV, scattering angle =5º). (a) The solid line is the projection of the 50% surface perpendicular to the energy axis, and the dashed lines are the intersection of the function with the planes $\delta\omega = 0$ and $\delta\omega = 3$ meV. The $\delta Q_{//}$ axis is parallel to $\underline{k}_I$. (b) The projection of the 50% surface perpendicular to $\underline{k}_I$.

3. TESTING THE RESOLUTION FUNCTION

3.1 Monitor widths

HET has two monitors in the direct beam downstream of the chopper. The first is almost immediately behind the chopper so the moderator pulse width will contribute negligably to the pulse width because there is very little distance over which the transmitted spread of energies can cause the pulse to disperse. The second is 7.51m behind the chopper and so will include a moderator pulse width component. Each will also have components arising from the sweep of the chopper across the moderator face and the monitor. The expression for the pulse at the monitor position is the convolution

$$\phi(t) = \int M(t_m)A(y_a)P(t'_{ch})H(y)\,\delta(t-(a_1t_m + a_2y_a + a_3t'_{ch} + a_4y))\,dt_m dy_a dt'_{ch} dy$$

[9]

where $H(y)$ is a hat function with width equal to that of the monitor. The coefficients a_i linearly relate the deviation in time of arrival at the monitor, t, to the deviations t_m, y_a, t'_{ch}, y and the variance of $\phi(t)$ is (expressing the a_i explicitly)

$$\langle t^2 \rangle = \left(\frac{l_m}{l_0}\right)^2 \langle t_m^2 \rangle + \left(1+\frac{l_m}{l_0}\right)^2 \langle t_{ch}^2 \rangle + \left(1+\frac{l_m}{l_0}\left(1-\frac{\omega}{v}(l_0+l_m)\tan\vartheta_m\right)\right)^2 \frac{\langle y_a^2 \rangle}{\omega^2 (l_a+l_m)^2}$$
$$+\left(1+\frac{l_m}{l_0}\left(1-\frac{\omega}{v}(l_0-l_a)\tan\vartheta_m\right)\right)^2 \frac{\langle y^2 \rangle}{\omega^2 (l_a+l_m)^2} \qquad [10]$$

Here l_m is the distance from the chopoper to the monitor, v the neutron speed and ϑ_m the angle the moderator face makes with the axis of the spectrometer. The last two terms in the equation are determined by the spectrometer geometry, as are the coefficients of the first two terms; the only uncertainties are the moderator and chopper pulse widths. Monitor_2 therefore allows the chopper pulse width to be checked against calculation, and monitor_3 will give the moderator pulse width once the chopper width is known.

The monitor widths in about 30 runs with incident energies between 130meV and 1000meV were measured with the HET Fermi chopper designed for use at high energies. Monitor_2 peaks were fitted by a Gaussian as each component (other than the moderator term) of equation 10 is comparable and arise from symmetric functions, whereas monitor_3 peaks were fitted by a Gaussian convoluted with the chi-squared function of equation 6. All the widths in monitor_2 agreed to 2% with values calculated using equation 10 with $\langle t'^2_{ch} \rangle$ calculated from the design values for the chopper slit width, radius of curvature and diameter (see figure 3). However, the widths in monitor_3 were systematically larger than calculated using equation 10. To reproduce the observed widths it was necessary to parametrise the decay constant τ as

$$\tau = \tau_0 + \frac{1}{\Sigma_{eff} v} \qquad [11]$$

with τ_0=0.35μs and Σ_{eff} =88m^{-1}. From the density of hydrogen in the moderator one would expect in the epithermal region $\Sigma \approx 150\text{m}^{-1}$. Typically, the observed moderator pulse width is about twice the calculated value.

3.2 Elastic scattering from vanadium

Now that the calculated chopper width has been confirmed and an empirical model for the moderator width determined, there no uncertain quantities appear in the calculation of the covariance matrix $C_{\alpha\beta}$. The element $C_{44} \equiv \langle \delta\omega^2 \rangle$ gives the variance of the elastic

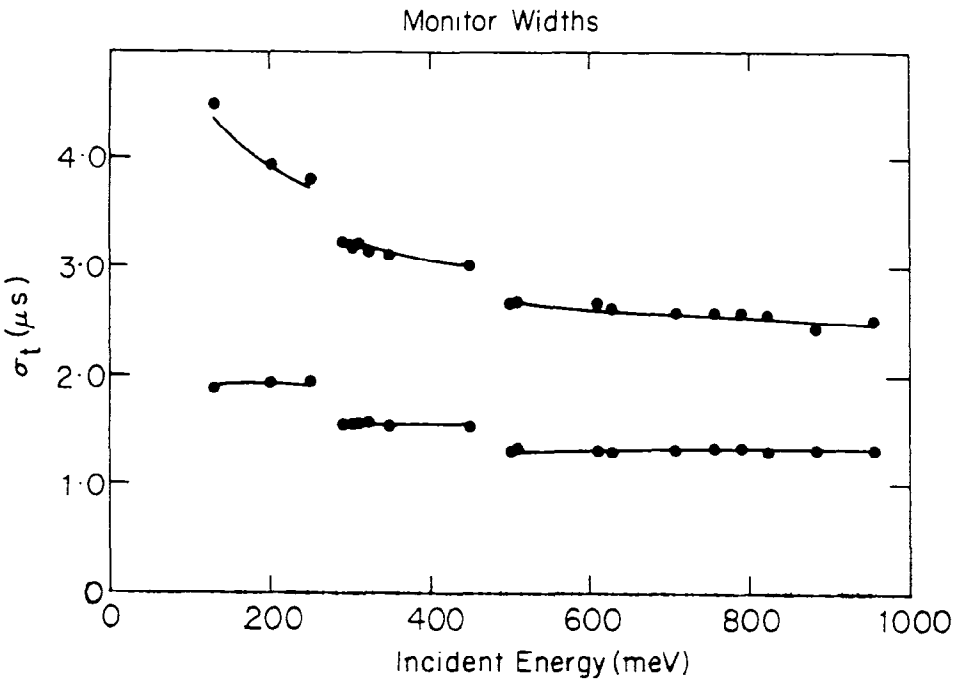

Figure 3: Experimental and calculated widths for monitor_2 (lower lines) and monitor_3 (upper lines). The discontinuities correspond to different chopper frequencies. Error bars on the fitted peak widths are smaller than the marks.

incoherent scattering peak ("vanadium width"). The widths of 22 such peaks with incident energies between 250meV and 880meV were measured, in detectors 4m and 2.5m from the sample position, from vanadium or cobalt (which has a comparable incoherent cross-section). The calculated widths are generally 10-20% less than the experimental widths (table 1). The origin of this discrepancy must be due to an extra component introduced to the width in the detectors that is so far unaccounted for, yet the calculation already includes the effect of sample size, detector thickness and focussing effects. One possibility is a "jitter" in the discrimination electronics of the detectors, which are ^{3}He gas tubes, but which is not present in that of the monitors, which are made from beads of ^{6}Li-doped scintillator glass on a wire grid. Further convolving the detector peaks widths with a function with standard deviation 1.3μs would give an excellent fit. The same effect and magnitude would also explain the observed discrepancy [6] between peaks widths in a gas tube and scintillator detector in the same position on the eVS spectrometer at ISIS.

4. SIMULATION OF MAGNETIC SCATTERING DATA FROM A SINGLE CRYSTAL [7]

This section describes an example of the application of the resolution function to understand some real data. MnCu(10%) is an itinerant antiferromagnet which orders three dimensionally. Near the zone centre the spin wave dispersion relation is expected to be approximately linear in reduced wavevector, $\omega(q) = \sqrt{\Delta^2 + (Dq)^2}$, with linear damping

Incident Energy (meV)	Chopper frequency (Hz)	Sample to detector (m)	Detector width (Standard deviation) (μs) Experimental	Calculated	Error (%)	missing width (μs)
Vandium data						
252	400	4 m	3.47	3.32	4	1.0
		2.5 m	3.20	2.92	9	1.3
303	500	4 m	3.08	2.86	7	1.1
		2.5 m	2.64	2.49	6	0.9
501	600	4 m	2.93	2.38	19	1.7
		2.5 m	2.53	2.07	18	1.4
629	600	4 m	2.60	2.31	11	1.2
		2.5 m	2.37	2.02	15	1.2
755	600	4 m	2.49	2.27	9	1.0
		2.5 m	2.64	2.00	24	1.7
884	600	4 m	2.60	2.23	14	1.3
		2.5 m	2.43	1.97	19	1.4
Cobalt data						
304	500	4 m	3.09	2.86	7	1.2
		2.5 m	2.86	2.49	13	1.4
501	600	4 m	2.76	2.38	14	1.4
		2.5 m	2.53	2.07	18	1.5
629	600	4 m	2.59	2.31	11	1.2
		2.5 m	2.48	2.02	18	1.4
755	600	4 m	2.78	2.27	18	1.6
		2.5 m	2.43	2.00	18	1.4
884	600	4 m	2.60	2.23	14	1.3
		2.5 m	2.53	1.97	22	1.6

Table 1

$\Gamma = \Gamma_0 + \Gamma_1 q$. Here Δ is the gap at zero wavevector and D the spin wave stiffness. Near the zone boundary calculations of the generalised magnetic susceptibility indicate that the dispersion relation becomes approximately flat. A highly simplified model is to assume the small q dispersion relation up to a cut-off value q^*, beyond which the frequency and damping have the values at q^*. To ensure sufficient statistics it is necessary to add several adjacent detectors together, which degrades $\underline{Q}$ resolution perpendicular to $\underline{k_F}$ to a value comparable to the vertical resolution. It is important to include this resolution to understand the data, and HETSIM was used to convolve the resolution function with the proposed dispersion relation.

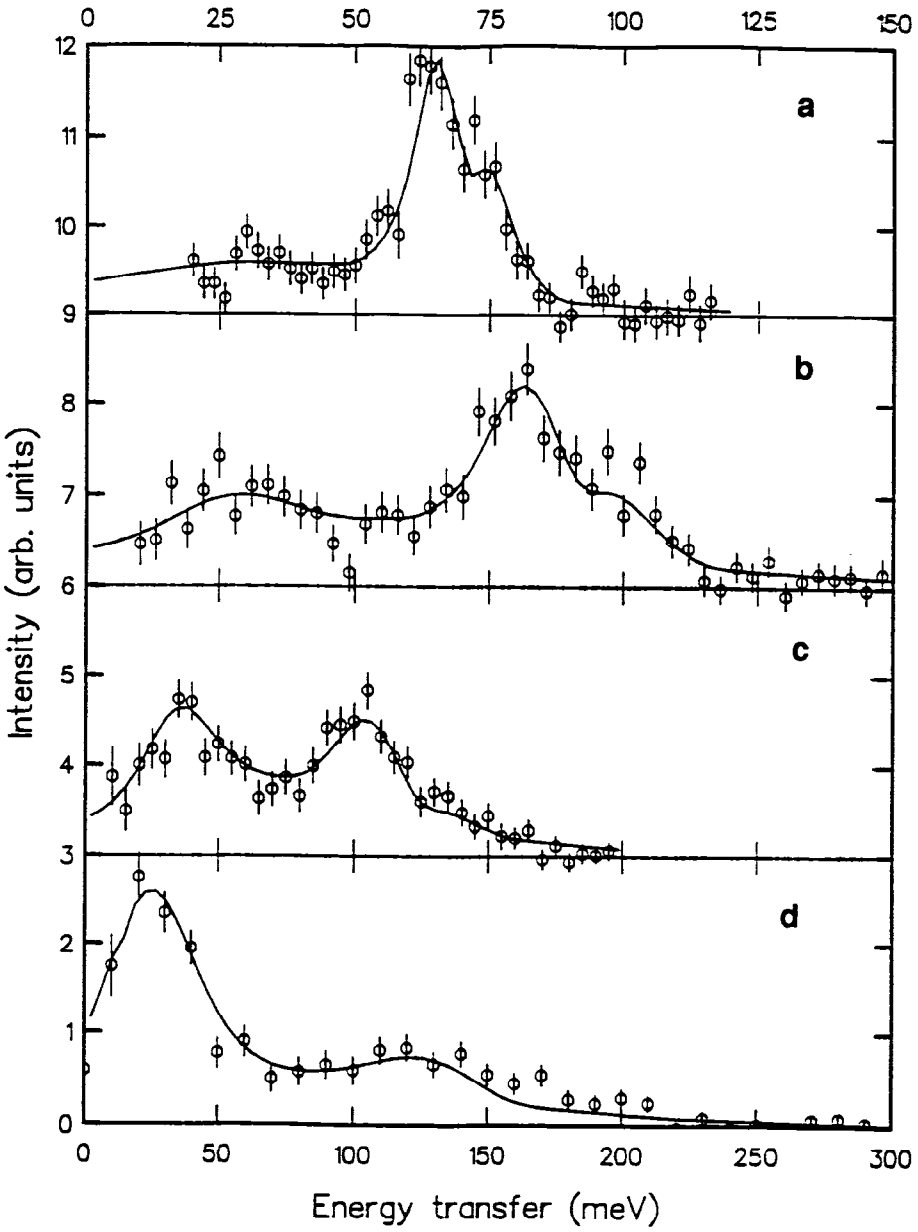

Figure 4: Measured spectra in the HET low angle detectors for MnCu(10%) in the [100]/[010] scattering plane. The values of E_I and ψ (the angle of [100] to $\underline{k}_I$) are (a) 157meV, 29.7°, (b) 262meV, 23.1°, (c) 443meV, 22.6°, (d) 813meV, 11.9°. The solid lines are the model calculations described in section 4.

Simulation of data obtained at several incident neutron energies, for which the trajectory in $(\underline{Q},\omega)$-space intersects the dispersion relation at different points, is shown in figure 4. The lower energy data is well explained using values of $\omega, \Delta, D, \Gamma_0$ and Γ_1 obtained from scattering data up to 60meV on a triple-axis spectrometer, but for the model to be consistent with tha data at high energies a cut-off wavevector q^*=0.8Å^{-1} corresponding to ω^*=190meV is required. The resulting simulation agrees closely with the data.

5. SUMMARY

The resolution function for HET and its sister instrument MARI has been calculated in a form suitable for high energy neutron experiments. Examination of monitor lineshapes and linewidths show that the calculated chopper pulse width agrees well with experiment, but that the HET moderator pulse width is considerably longer than expected from the water moderator. With the parametrisation of the moderator obtained from monitor data, the predicted widths in the detectors from elastic vanadium scattering are still 15% less than the experimental widths, but this discrepancy can be accounted for by 'jitter' in the detector electronics. The convolution of the resolution function with a model dispersion relation gives good agreement with magnetic scattering from a single crystal.

REFERENCES

[1] A.D. Taylor, B.C. Boland, Z.A. Bowden, T.J.L. Jones, Rutherford Appleton Laboratory Report RAL-87-012 (1987)
[2] K.H. Beckurts and K. Wirtz, 'Neutron Physics' (Springer Verlag, Berlin, 1964)
[3] M. Marseguerra and G. Pauli, Nucl.Instr. and Meth. **4** (1959) 140
[4] M.J. Cooper and R. Nathans, Acta Cryst. **23** (1967) 357
[5] P.W. Mitchell, R.A. Cowley and S.A. Higgins, Acta Cryst. **A40** (1984) 152
[6] J. Mayers, private communication
[7] J.A. Fernandez-Baca, M.E.Hagen, R.M. Nicklow, T.G.Perring, Y.Tsunoda, J.Appl. Phys. **73** (1993) 6548